Effects of Substituting Sr^{2+} and Ba^{2+} for Ca^{2+} on the Structural Properties and Photocatalytic Behaviors of $CaIn_2O_4$

Junwang Tang,*,† Zhigang Zou,‡ and Jinhua Ye*,†

Ecomaterials Center, National Institute for Materials Science (NIMS), 1-2-1 Sengen, Tsukuba, Ibaraki 305-0047, Japan, and Ecomaterials and Renewable Energy Research Center (ERERC), Nanjing University, 22 Hankou Road, Nanjing 210093, China

Received December 26, 2003. Revised Manuscript Received February 12, 2004

MIn_2O_4 (M = Ca, Sr, Ba) semiconductors were synthesized by a simple solid-state reaction and characterized by X-ray diffraction (XRD), scanning electron microscope (SEM), and UV−visible spectrometer. The substitution effects of M^{2+} ion on the structural and photocatalytic properties for methylene blue (MB) dye degradation were first investigated systematically. It was found that when M goes from Ca to Ba, the crystal structure of these materials changed from orthorhombic to monoclinic structure, resulting in a systematic variation of the photophysical and photocatalytic properties of these materials. Among these semiconductors, $CaIn_2O_4$ showed the highest activity in a wide wavelength range of visible light up to 580 nm. The representative product of the MB degradation, SO_4^{2-}, was examined and indicated that MB was partially mineralized on MIn_2O_4 (M = Ca, Sr, Ba). The pH value of MB solution and the synthesized temperature of the photocatalyst were also found to have a significant effect on the photocatalytic activity of these materials. The possible reaction pathway was suggested.

1. Introduction

Photocatalytic degradation of organic compounds for the purpose of purifying dye wastewater from industries and households has attracted much attention in recent years.[1−5] The desired effect in this process is that photogenerated holes in a semiconductor photocatalyst oxidize the organic pollutant via intermediate products to inorganic substances, such as Cl^-, SO_4^{2-}, NO_3^-, and so on. The dye wastewater contains many dyes contaminants.[6] Among them, methylene blue (MB) is often considered as a model dye contaminant.[1,6−8] Although there were numerous reports of photocatalytic MB degradation over the TiO_2-based photocatalysts, most of the studies were performed under UV light irradiation.[6,7] Recently, Zhao et al. reported that some dyes could be degraded under visible light irradiation on TiO_2 by a self-photosensitized process;[9] however, MB is exclusive. Up to now, there were only few reports of MB dye degradation under visible light irradiation, like that of Asahi et al. with a reduced TiO_x ($TiO_{2-x}N_x$) or Li et al. with a Au−TiO_2 photocatalyst.[1,10] Furthermore, the efficiency is limited by the light absorption characteristics of the TiO_2-based photocatalysts. To utilize efficiently the solar or artificial light irradiation, it is indispensable to develop a new visible-light-driven photocatalytic material with high activity.

So far, a number of photocatalysts containing InO_6 like $AgInW_2O_8$ and $InMO_4$ (M = Ta, Nb, V) were reported to show an activity for water splitting under light irradiation,[11,12] where the InO_6 octahedral chains were considered to favor a possible mobility of charge carriers and enhance the photocatalytic activity. Very recently, we found that MB could be degraded on $CaIn_2O_4$ under visible light irradiation.[13] Substitution of Ca^{2+} with other elements, such as Sr^{2+} or Ba^{2+}, might induce a slight modification of crystal structure because of the different ion radii, resulting in dramatic influence

* To whom correspondence should be addressed. Fax: 80-298-59-2601. E-mail: jinhua.ye@nims.go.jp or tang.junwang@nims.go.jp.
† NIMS.
‡ Nanjing University.

(1) Asahi, R.; Morikawa, T.; Ohwaki, T.; Aoki, K.; Taga, Y. *Science* **2001**, *293*, 269.
(2) Hoffman, M. R.; Martin, S. T.; Choi, W.; Bahnemann, D. W. *Chem. Rev.* **1995**, *95*, 69.
(3) Mills, A.; Hunte, S. L. *J. Photochem. Photobiol. A: Chem.* **1997**, *108*, 1.
(4) Hu, C.; Tang, Y.; Yu, J.; Wong, P. *Appl. Catal. B* **2003**, *40*, 131.
(5) Yamashita, H.; Harada, M.; Misaka, J.; Takeuchi, M.; Ikeue, K.; Anpo, M. *J. Photochem. Photobiol. A Chem.* **2002**, *148*, 257.
(6) Houas, A.; Lachheb, H.; Ksibi, M.; Elaloui, E.; Guillard, C.; Herrmann, J. M. *Appl. Catal. B* **2001**, *31*, 145.
(7) For recent results, see: Belhekar, A. A.; Awate, S. V.; Anand, R. *Catal. Commun.* **2002**, *3*, 453. Fernandez, J.; Kiwi, J.; Lizama, C.; Freer, J.; Baeza, J.; Mansilla, H. D. *J. Photochem. Photobiol. A: Chem.* **2002**, *151*, 213. Tsumura, T.; Kojitan, N.; Izumi, I.; Iwashita, N.; Toyoda, M.; Inagaki, M. *J. Mater. Chem.* **2002**, *12*, 1391. Zhang, T.; Oyama, T.; Aoshima, A.; Hidaka, H.; Zhao, J.; Serpone, N. *J. Photochem. Photobiol. A: Chem.* **2001**, *140*, 163.
(8) Li, F. B.; Li, X. Z. *Appl. Catal. A* **2002**, *228*, 15.
(9) Zhao, W.; Chen, C.; Li, X.; Zhao, J.; Hidaka, H.; Serpone, N. *J. Phys. Chem. B* **2002**, *106*, 5022. Wu, T.; Liu, G.; Zhao, J.; Hidaka, H.; Serpone, N. *J. Phys. Chem. B* **1998**, *102*, 5845. Wu, T.; Liu, G.; Zhao, J.; Hidaka, H.; Serpone, N. *J. Phys. Chem. B* **1999**, *103*, 4862.
(10) Li, X. Z.; Li, F. B. *Environ. Sci. Technol.* **2001**, *35*, 2381.
(11) Tang, J.; Zou, Z.; Ye, J. *J. Phys. Chem. B* **2003**, *107*, 14265.
(12) Ye, J.; Zou, Z.; Oshikiri, M.; Matsushita, A.; Shimoda, M.; Imai, M.; Shishido, T. *Chem. Phys. Lett.* **2002**, *356*, 221. Zou, Z.; Ye, J.; Arakawa, H. *Chem. Phys. Lett.* **2000**, *332*, 271.
(13) Tang, J.; Zou, Z.; Yin, J.; Ye, J. *Chem. Phys. Lett.* **2003**, *382*, 175.

10.1021/cm0353815 CCC: $27.50
Published on Web 03/30/2004

on the mobility of the charge carrier. The mobility of the charge carrier is closely relevant to the photocatalytic activity of a material, because it affects the probability of electrons reaching the reaction active sites.[14] Few reports exist on the effects of changing the ionic radius of the materials on their photocatalytic activity for organic decomposition and structural properties. Here, a series of MIn_2O_4 (M = Ca, Sr, Ba) were synthesized, which all contain InO_6 octahedral chains. Sato et al. found some of these materials had an activity for water splitting under UV light irradiation.[15] In the present work, a systematic investigation on the photocatalytic and structural properties of MIn_2O_4 (M = Ca, Sr, Ba) was performed. Their activity to purify dye wastewater was observed in detail under visible light irradiation, where MB was selected as a model dye contaminant. The effects of material preparation and reaction condition on the photocatalytic and structural properties of MIn_2O_4 (M = Ca, Sr, Ba) were also investigated. A possible photocatalytic pathway was suggested on the basis of the understandings of the photocatalytic and photophysical properties of MIn_2O_4 (M = Ca, Sr, Ba).

2. Experimental Section

2.1. Materials. MIn_2O_4 (M = Ca, Sr, Ba) semiconductors were prepared by a solid-state reaction method. MCO_3 (M = Ca, Sr, Ba) and In_2O_3 were purchased from Wako Pure Chemical Industries, Ltd., and then mixed with 1:1 molar ratio in an ethanol solution. The mixtures were dried at 353 K for 5 h and calcined at 1173 K for 12 h. Then, the calcined samples were reground vigorously and blended. Finally, they were sintered at 1323 K for 12 h in air. To observe the effect of sintered temperature on the physical and photoactive properties of the material, another $CaIn_2O_4$ sample was sintered at 1273 K for 34 h in air and designated as $CaIn_2O_4$-1273.

2.2. Characterization. The crystal structure of the materials was determined by a powder X-ray diffraction (XRD) method (volt, 35 kV; current, 300 mA), where a copper target was used (Cu Kα radiation, λ = 0.154 178 nm). UV−visible diffuse reflectance spectra of the samples were measured by UV−visible spectrometer (UV-2500, Shimadzu, Japan). The surface area of the samples was determined by BET measurement on nitrogen adsorption at 77 K (Micromeritics Automatic Surface Area Analyzer Gemini 2360, Shimadzu, Japan) after the pretreatment at 573 K for 2 h. Scanning electron microscopy (SEM) images of the samples were obtained in a JEOL JSM 5400 operated at 15 kV.

2.3. Photocatalytic Behavior. The optical system used for the photocatalytic reaction consisted of a 300 W Xe arc lamp, which focused the light onto the reaction cell, a cutoff filter (providing the visible light of different wavelength), and a water filter (preventing from thermal catalytic effect). The photocatalytic reaction was carried out with 0.3 g of powdered photocatalysts suspended in 100 mL of MB solution in a Pyrex glass cell. MB solution was prepared with MB powder and distilled water. Its concentration was about 15.3 mg/L. Titania was commercially available Degussa P-25. All experiments were conducted at room temperature in air. The slurry samples including the photocatalyst and MB solution were separated by syringe-driven filter unit (Millex, Millipore Corp.). The solution was analyzed by a UV−visible spectrometer (UV-2500, Shimadzu, Japan).[6,8] The product of MB degradation was determined by an ion chromatograph with a conductivity detector (LC-10ADsp Ion Chromatograph, Shimadzu).

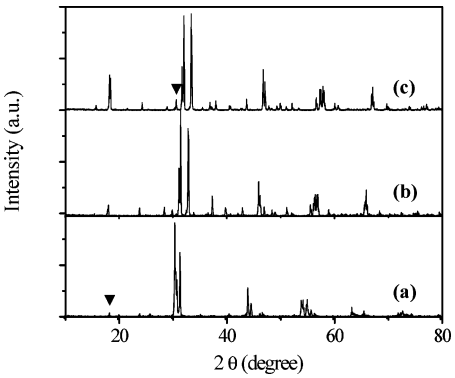

Figure 1. XRD patterns of MIn_2O_4 (M = Ca, Sr, Ba): (a) $BaIn_2O_4$, (b) $SrIn_2O_4$, and (c) $CaIn_2O_4$. (▼): In_2O_3 peak.

Table 1. Lattice Parameters of Different Semiconductors

semicond	ionic radii of M^{2+} (nm)	crystal structure	space group	lattice parameter (nm)	cell volume (nm^3)
$CaIn_2O_4$	0.099	orthorhombic	*Pnam*	a = 0.9650 b = 1.1305 c = 0.3213	0.3505
$SrIn_2O_4$	0.113	orthorhombic	*Pnam*	a = 0.9828 b = 1.1493 c = 0.3262	0.3685
$BaIn_2O_4$	0.135	monoclinic	*P*21/*a*	a = 1.4432 b = 2.0769 c = 0.5826 β = 110.02°	1.6408

3. Results and Discussion

3.1. Structural and Physical Properties. The XRD patterns of MIn_2O_4 are shown in Figure 1. From the profile simulation on the basis of the previous works, all these oxides are basically single phases, except a small amount of In_2O_3 impurity.[16,17] The lattice parameters of these materials were refined by the least-squares method. The results of the refinement are represented in Table 1. With increasing the ionic radii of M (from Ca to Sr to Ba), not only lattice parameters but also crystal structure types of the materials changed. XRD analysis revealed that $CaIn_2O_4$ and $SrIn_2O_4$ have a similar crystal structure, which belongs to an orthorhombic symmetry. When Ca^{2+} was replaced by Sr^{2+}, all the peaks in the XRD patterns shifted toward a smaller degree, indicating an increase in the lattice parameters of these materials, in agreement with the above-mentioned refinement results. On the other hand, $BaIn_2O_4$ has a monoclinic crystal structure.[17] The structural features of $CaIn_2O_4$ and $SrIn_2O_4$ (see Figure 2a) are the presence of two kinds of distorted InO_6 octahedra.[16,18] The InO_6 octahedra are connected to form the pentagonal prism tunnel by sharing corner and edge, and Ca or Sr is located in the middle of the tunnel. $BaIn_2O_4$ consists of several kinds of InO_x polyhedra (see Figure 2b), including the distorted InO_6 octahedra. InO_x polyhedra are connected to form a network by sharing corner, edge, and side, and Ba is located in the network.

It's known that key factors controlling a photocatalytic reaction involve mainly the abilities of (1) adsorption

(14) Zou, Z.; Ye J.; Arakawa, H. *Chem. Mater.* **2001**, *13*, 1765.
(15) Sato, J.; Saito, N.; Nishiyama, H.; Inoue, Y. *J. Phys. Chem. B* **2001**, *105*, 6061. Sato, J.; Saito, N.; Nishiyama, H.; Inoue, Y. *J. Phys. Chem. B* **2003**, *107*, 7965/7970.
(16) Von Schenck, V. R.; Muller-Buschbaum, Hk. *Anorg. Allg. Chem.* **1973**, *398*, 24.
(17) Lalla, A.; Mueller-Buschbaum, H. *J. Less-Common Met.* **1989**, *154*, 233.
(18) Sato, J.; Saito, N.; Nishiyama, H.; Inoue, Y. *Chem. Lett.* **2001**, 868.

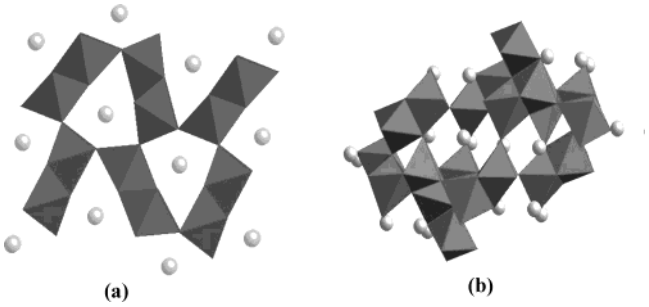

Figure 2. Schematic crystal structure of (a) $SrIn_2O_4$ and (b) $BaIn_2O_4$.

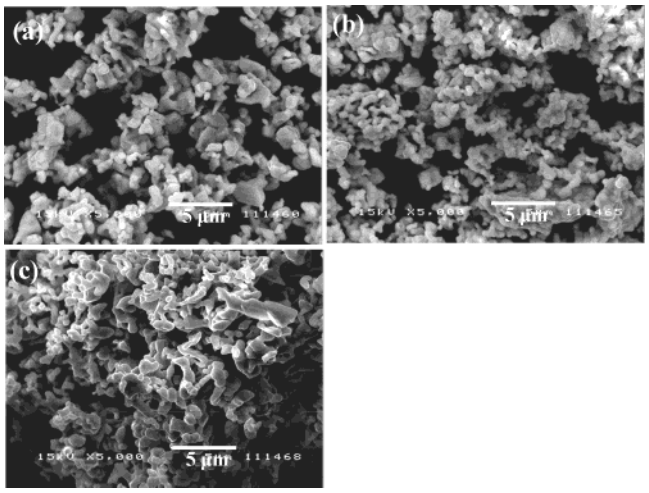

Figure 3. SEM images of (a) $CaIn_2O_4$ synthesized at 1323 K, (b) $SrIn_2O_4$ synthesized at 1323 K, and (c) $CaIn_2O_4$ synthesized at 1273 K.

Table 2. Physical Properties of Different Semiconductors and Their Photocatalytic Behaviors under Visible Light Irradiation (λ > 420 nm)

semiconductor	surface area (m^2/g)	MB adsorption (mg of MB/ g of catalyst)	initial rate of MB degradn per surf. area (mg/h·m^2)	SO_4^{2-} concn (mg/L)
P-25	49.41	1.08	2.75×10^{-2}	0
$CaIn_2O_4$-1273	1.27		9.47	
$CaIn_2O_4$	0.86	0.38	8.33	2.66
$SrIn_2O_4$	0.84		3.10	1.87
$BaIn_2O_4$	0.79		2.13	1.30

of the reactant on the surface of a material and (2) light absorption by the material as well as the migration of the light-induced electrons and holes. The former is strongly dependent on the surface area of the material. The latter is relevant to the electronic structure characteristics of the material. Table 2 lists the BET surface area of MIn_2O_4 and the most well-known TiO_2 photocatalyst P-25. Compared to the large surface area of P-25 (49.41 m^2/g), that of these examined oxides is much smaller (~0.8 m^2/g). Figure 3 represents the SEM images of the samples. It is clear that the particle size of the sample is about 1 μm, in good agreement with their measured surface area. As a typical example, the adsorbed amount of MB on $CaIn_2O_4$ was measured after keeping the equilibrium for 1 h in the adsorption−desorption process. The adsorption amount of MB over P-25 was also measured. The former was only 0.38 mg of MB/g of catalyst, the latter was 1.08 mg of MB/g of catalyst. These results were consistent with the surface areas of the two semiconductors.

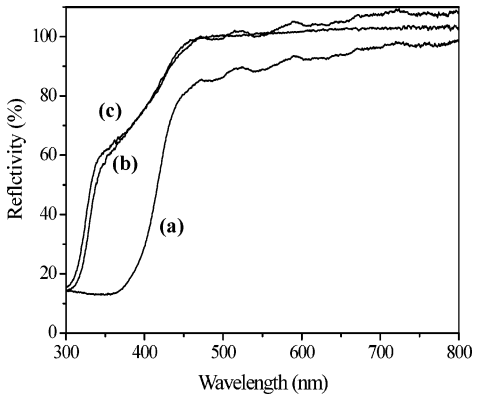

Figure 4. Diffuse reflectance spectra of (a) $BaIn_2O_4$, (b) $SrIn_2O_4$, and (c) $CaIn_2O_4$.

The photoabsorption abilities of these materials were detected by UV−visible diffuse reflectance spectra (UV−vis DRS). The spectra are shown in Figure 4. All MIn_2O_4 presented the photoabsorption properties from UV light region to visible light region shorter than 480 nm. Although the fundamental aspect among them was similar in the visible light region, there is the slight difference of profile for MIn_2O_4, which was probably decided by the structural difference due to the different ionic radii of M^{2+}. The color of these oxides was yellowish, as predicted from their photoabsorption spectra, which are correlated with their band structure. The band structure of a transition metal oxide is generally defined by the d level of the transition metal and O 2p level.[19] However, for the metal oxides containing a metal ion with d^{10} electronic configuration, the conduction band is not formed by its d level. Theoretical calculations showed that the band features of the indium oxides with InO_6 octahedra were dominated by the O 2p level and the In 5s level.[20,21] Therefore, the band structures of MIn_2O_4 were suggested to be composed of In 5s levels (conduction band, CB) and O 2p levels (valence band, VB). The photoabsorption ability of these photocatalysts was due to the electronic excitation from the O 2p orbital to the In 5s orbital. For a crystalline semiconductor, it was shown that the optical absorption near the band edge follows the equation[22]

$$a = A\frac{(h\nu - E_g)^{n/2}}{h\nu}$$

where a, ν, E_g, and A are absorption coefficient, light frequency, band gap, and a constant, respectively. Among them, n decides the characteristics of the transition in a semiconductor. According to the equation, the values of n for these indium oxides were determined to be 4 from the data in Figure 4. This means that the optical transitions for these indium oxides are all indirectly allowed.

3.2. Photocatalytic Behaviors. The MB degradation over these materials under visible light irradiation (wavelength λ > 420 nm) was investigated first. Figure

(19) Scaife, D. E. *Sol. Energy* **1980**, *25*, 41.
(20) Odaka, H.; Iwata, S.; Taga, N.; Ohnishi, S.; Kaneta, Y.; Shigesato, Y. *Jpn. J. Appl. Phys.* **1997**, *36* (9a), 5551.
(21) Schinzer, C.; Heyd, F.; Mater, S. F. *J. Mater. Chem.* **1999**, *9*, 1569.
(22) Knox, A. B. *Trans. Br. Ceram. Soc.* **1967**, *66*, 85. Butler, M. A. *J. Appl. Phys.* **1977**, *48*, 1914.

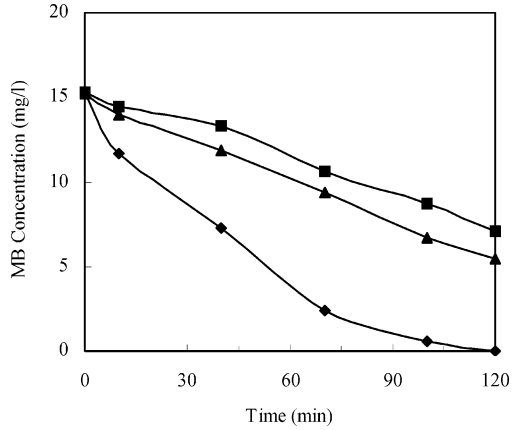

Figure 5. MB degradation over MIn_2O_4 (M = Ca, Sr, Ba) semiconductors under visible light (λ > 420 nm) at room temperature in air: ■, $BaIn_2O_4$; ▲, $SrIn_2O_4$; and ◆, $CaIn_2O_4$.

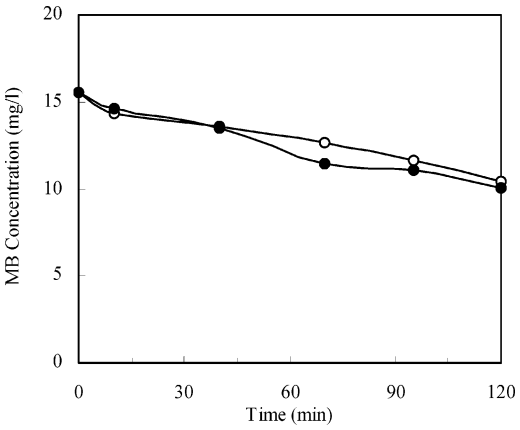

Figure 6. MB photolysis (○) and MB degradation over P-25 (●) under visible light (λ > 420 nm) at room temperature in air.

5 represents the variation of MB concentration vs reaction time over a series of MIn_2O_4. It was obvious that MB was degraded over all photocatalysts under visible light irradiation. However, the photocatalytic activities of these catalysts were distinct from each other. As shown in this figure, the most interesting result was the complete degradation of MB over $CaIn_2O_4$ after 120 min of irradiation. $SrIn_2O_4$ showed the intermediate ability and $BaIn_2O_4$ the lowest one. This activity difference among the three photocatalysts was possibly due to their variation of the above-mentioned structural characteristics.

As a comparison, MB degradation over P-25 and MB photolysis without any photocatalyst (namely, the photobleaching of MB) were also observed under the same condition. The results are shown in Figure 6. It could be seen that the variation of MB concentration over P-25 was similar to that in MB photolysis. This suggested that P-25 was inactive to MB photocatalytic degradation under visible light irradiation, which was consistent with the results of Asahi et al.[1] Altogether, MB degradation over the MIn_2O_4 photocatalysts was remarkable, whereas the photobleaching of MB and MB degradation over TiO_2 were negligible under visible light irradiation (Table 2), although alizarion red dye, orange II, and rhodamine B dye were reported to be degraded over TiO_2 under visible light based on a dye-photosensitized process.[9,23,24] The color of the MB solution was

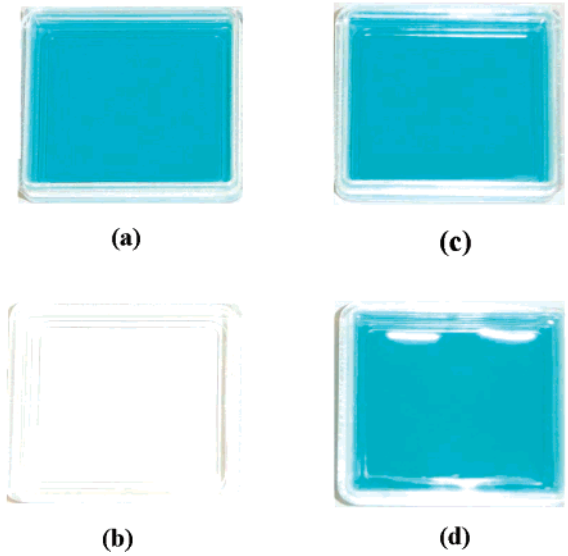

Figure 7. Photos of the solution before and after the photocatalytic reactions: (a) MB solution before the reaction, (b) MB solution after the reaction over $CaIn_2O_4$, (c) MB solution before the reaction, and (d) MB solution after the reaction over P-25.

also observed during the photocatalytic reaction (Figure 7). After irradiation for 120 min, the color changed from deep blue to colorless for $CaIn_2O_4$ and changed a little for P-25. The results were in good agreement with the activities of the photocatalysts.

The anion SO_4^{2-} is one of the main products of MB mineralization. It can be used to distinguish if MB was degraded. The SO_4^{2-} ion concentration in the solution was determined by ion chromatography and is listed in Table 2. It was 2.66 mg/L after the 120 min photocatalytic reaction over $CaIn_2O_4$ (namely, nearly 60% of MB was mineralized), 1.87 mg/L over $SrIn_2O_4$ (nearly 42% of MB was mineralized), 1.30 mg/L over $BaIn_2O_4$ (nearly 30% of MB was mineralized), and 0 mg/L over P-25. These results indicated that MB was degraded over MIn_2O_4 rather than bleached under visible light irradiation.

To examine the photocatalytic stability of the semiconductors, the used $CaIn_2O_4$ photocatalyst was employed again to degrade MB under visible light (λ > 420 nm). It was found that the used $CaIn_2O_4$ photocatalyst showed an activity similar to that of the fresh one, implying that the photocatalytic activity of $CaIn_2O_4$ was repeatable. XRD patterns analysis of MIn_2O_4 before and after photocatalytic reaction also showed that the crystal structure of the semiconductor did not change, suggesting that MIn_2O_4 were stable in the photocatalytic reaction.

3.3. Effects of Reaction Condition and Material Preparation. The pH value is a complex parameter, since it is related to the state of the material surface, which affects the adsorption of MB on the material.[6] The effect of pH value on the photoreaction was investigated over $BaIn_2O_4$, and the results are represented in Figure 8. In the alkaline solution (pH was nearly 10), the activity of $BaIn_2O_4$ was higher than that in the neutral

(23) Liu, G.; Wu, T.; Zhao, J.; Hidaka, H.; Serpone, N. *Environ. Sci. Technol.* **1999**, *33*, 2081.
(24) Qu, P.; Zhao, J.; Shen, T.; Hidaka, H. *J. Mol. Catal. A: Chem.* **1998**, *129*, 257.

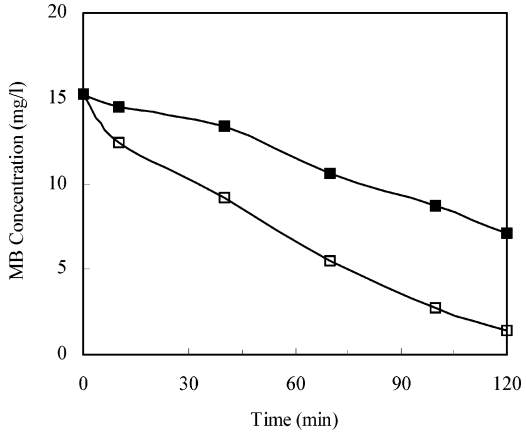

Figure 8. MB degradation with different pH value over $BaIn_2O_4$ under visible light irradiation (λ > 420 nm); ■, pH value approximately 7; □, pH value approximately 10.

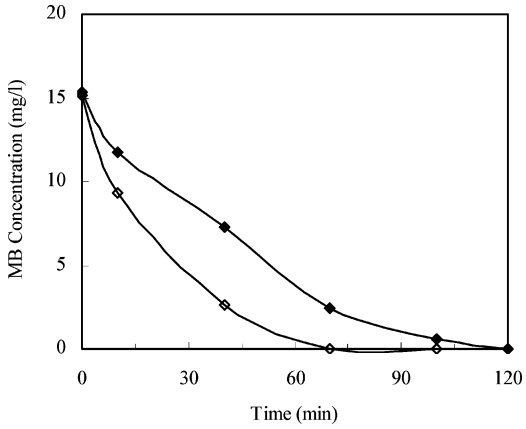

Figure 9. MB degradation over $CaIn_2O_4$ synthesized at (◆) 1323 K and (◇) 1273 K under visible light irradiation (λ > 420 nm).

solution (pH was nearly 7), which was consistent with the results obtained by Houas et al. under UV light irradiation,[6] indicating that the pH value of the solution obviously affected the activity of the photocatalyst. Because MB dye is in its cationic form in the solution, an alkaline solution is beneficial to MB adsorption on the material surface. Therefore, it is reasonable that the activity of the semiconductor was enhanced in the alkaline media. Similar results were reported by Zhang et al. for the photocatalytic decomposition of eosin.[25]

The effects of the synthesis temperature of $CaIn_2O_4$ on its activity are shown in Figure 9. The results revealed that the temperature during the synthesis of the material clearly affected its photocatalytic activity. The surface area and SEM images of $CaIn_2O_4$ synthesized at different temperature were observed and are listed in Table 2 and Figure 3, respectively. The particle size of the two samples looks to be similar, while the surface area of $CaIn_2O_4$ synthesized at 1273 K ($CaIn_2O_4$-1273) was 1.27 m^2/g and that synthesized at 1323 K was only 0.86 m^2/g. Hence, the synthesis temperature of the material obviously affected its surface area and then its photocatalytic activity (See the initial reaction rate in Table 2). The surface area of the present material was nearly 1 m^2/g, which was 2% of the surface area of P-25.

(25) Zhang, F.; Zhao, J.; Shen, T. Hidaka, H.; Pelizzetti, E.; Serpone, N. *Appl. Catal. B* **1998**, *15*, 147.

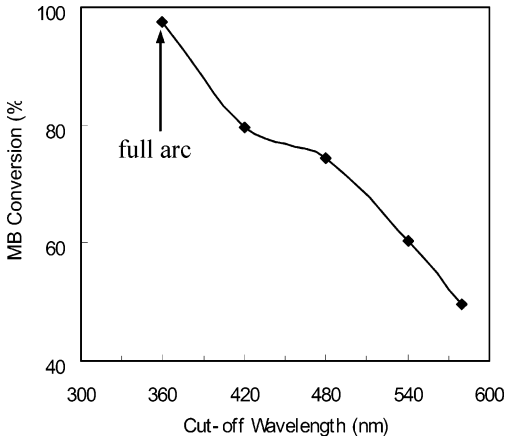

Figure 10. Wavelength dependence of MB conversion with different cutoff filters after light irradiation for 70 min over $CaIn_2O_4$ at room temperature in air.

Table 3. SO_4^{2-} Ion Concentration in the Solution after MB Degradation over $CaIn_2O_4$ with Different Cutoff Filters

filter (nm)	420	480	540	580
SO_4^{2-} (mg/L)	2.66	2.20	1.65	1.10

Considering the great effect of the surface area of the sample on its activity, the nanosized materials with the very large surface area are being investigated further.

3.4. Wavelength Dependence and Reaction Pathway. The wavelength dependence of the photocatalytic activity of a semiconductor is often used to distinguish if the reaction is really driven by light. Here, the light wavelength (λ) dependence of MB degradation was observed from full arc (without filter) to $\lambda \geq 580$ nm using different cutoff filters (Figure 10). If a reaction is driven by light, the variation of the light wavelength will affect directly the amount of photons entering the reaction system and then the photocatalytic properties. In the present work, it is obvious that the variation of the photocatalytic properties over $CaIn_2O_4$ was closely relevant to that of light wavelength, suggesting that MB catalytic degradation over $CaIn_2O_4$ was truly driven by light. Meanwhile, the photocatalyst showed a very high photocatalytic activity both in the UV light region (nearly 100% MB degradation) and in the visible light region (nearly 80% MB degradation, λ > 420). Even when the cutoff filter of 580 nm was employed, the photocatalyst still kept a high activity, while Asahi et al. found that $TiO_{2-x}N_x$ lost its activity when the light wavelength was longer than 500 nm.[1] These results indicated that the photocatalyst had a novel photocatalytic performance under the wide visible light region. The SO_4^{2-} concentration in the solution was determined when changing the visible light wavelength. The results are listed in Table 3. The data were basically consistent with the results in Figure 10, which suggested that MB was mineralized clearly under visible light irradiation. Similar phenomena were also observed on the other samples in addition to $CaIn_2O_4$. However, their activity was much lower than that of $CaIn_2O_4$.

The photocatalytic reaction involves (1) the adsorption of the reactants, (2) the generation of photoelectrons and photoholes in the photocatalyst, and (3) the transfer of photogenerated charge carriers (including holes and electrons) and the utilization of the charge carriers by the reactants.[2,15] MIn_2O_4 showed the action of adsorbing

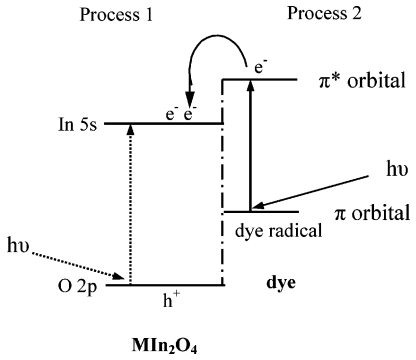

Figure 11. Possible pathway of the photoelectrons transfer excited by visible light irradiation, including process 1 (dotted line) and process 2 (solid line).

MB and the ability of absorbing visible light, which could cause the transition of the electrons from VB (O 2p) to CB (In 5s) in the photocatalysts. So it can be visualized that MB was degraded within a certain wavelength range of visible light over MIn_2O_4. Figure 4 showed that the light absorption by the oxides occurred dominantly when $\lambda < 480$ nm. Namely, MB can be photocatalytically degraded when the wavelength is shorter than 480 nm (process 1 in Figure 11).

Meanwhile, $CaIn_2O_4$ also showed the activity when the light wavelength was much longer than 480 nm, where it absorbed poorly the light radiation. It is well-known that MB dye can absorb the whole range of visible light, which is attributed to the ground state and the excited state of the dye.[26] So the materials absorbing light irradiation should be MB and MIn_2O_4 together in the present work. Among them, MB was the main material absorbing light irradiation when $\lambda \geq 480$ nm. MB photolysis results (in Figure 6) have revealed that MB without any photocatalysts was not degraded greatly under visible light irradiation. Therefore, the existence of MIn_2O_4 was indispensable for the photocatalytic degradation of MB, even if the light wavelength was longer than 480 nm. When $\lambda \geq 480$ nm, the photocatalytic origin was attributed to the photocatalysis of MIn_2O_4 assisted by MB dye adsorbed on the MIn_2O_4 surface. The detail of the origin was that MB dye absorbed the incident photon flux. Then the photogenerated electrons were transferred to the excited state of the dye owing to the intramolecular $\pi-\pi^*$ transition and the dyes were oxidized. The photoelectrons of the excited state were immediately injected into CB (In 5s level) of MIn_2O_4. Then, the photoelectrons in CB were captured by O_2 and the oxidized dyes were degraded via several intermediates (process 2 in Figure 11). The process might be similar to the surface sensitization of semiconductor via adsorbed dyes.[7,26,27] Altogether, process 1 (dotted line, the direct photocatalytic action of the photocatalysts) and process 2 (solid line, the photocatalytic action of the photocatalysts assisted by adsorbed MB dye) in Figure 11 would work when the light wavelength was shorter than 480 nm, while only process 2 worked when the light wavelength was longer than 480 nm.

In the present work, the variation of photocatalytic properties of MIn_2O_4 might be due to the radii difference of the M^{2+} ion (M = Ca, Sr, Ba), which influenced the crystal structures and the potential levels of the photocatalysts.[15] Alternatively, Kudo et al. found that substitution of M^{+5} (M = Ta, Nb) in $Sr_2M_2O_7$ greatly affected the mobility of the charge carrier.[28] Zou et al. also reported that the mobility of the electrons increased upon decreasing the ionic radii of M in Bi_2MNbO_7 (M = Al, Ga, In). Meanwhile, the photocatalytic activity of Bi_2MNbO_7 (M = Al, Ga, In) for H_2 evolution increased when decreasing the ionic radii of M.[14] In the present work, similar results were found for MB degradation on MIn_2O_4 (M = Ca, Sr, Ba). This means that the variation of photocatalytic properties of MIn_2O_4 might also be attributed to the effect of the mobility of the charge carriers caused by the radii difference of the M^{2+} ion (M = Ca, Sr, Ba). So, this research provided an understanding of the relationship between the ionic radii of M^{2+} and the photocatalytic activity of the semiconductor. Research of the intermediates in the process of MB dye degradation over these materials is in progress.

4. Conclusions

MIn_2O_4 (M = Ca, Sr, Ba) semiconductors were synthesized as the photoactive materials containing InO_6 octahedral structure. The crystal structure of these materials changed upon increasing of M^{2+} ionic radius, which resulted in a systematic variation of their photophysical and photochemical behaviors for MB dye degradation. Product analysis during MB degradation revealed that synthesized MIn_2O_4 were very active photocatalysts for MB mineralization under visible light irradiation, while MB photolysis and P-25 photocatalysis were negligible under the same condition. Especially, MB was degraded completely on $CaIn_2O_4$ after irradiating for 120 min over at a wide range of visible light irradiation up to 580 nm. A possible pathway of the photocatalytic reaction was suggested that involved the direct photocatalytic action of the semiconductors and the photocatalytic action of the semiconductors assisted by adsorbed MB dye. Altogether, the present work provides useful information on the pathway of photocatalytic dye degradation and synthesizing a promising photocatalytic material with high activity for dye wastewater treatment under visible light irradiation.

Acknowledgment. We acknowledge the Grant-in-Aid for the Creation of Innovations thorough Business-Academic-Public Sector Cooperation, Japan, for financial support. We thank Prof. Takehiko Matsumoto for his valuable discussion and Ms. Liqun Yang for her help in the experiment.

CM0353815

(26) Hara, K.; Sato, T.; Katoh, R.; Furube, A.; Ohga, Y.; Shinpo, A.; Suga, S.; Sayama, K.; Sugihara, H.; Arakawa, H. *J. Phys. Chem. B* **2003**, *107*, 597.

(27) Chatterjee, D.; Mahata, A. *J. Photochem. Photobiol. A: Chem.* **2002**, *153*, 199.

(28) Kudo, A.; Kato, H.; Nakagawa, S. *J. Phys. Chem. B* **2000**, *104*, 571.